Large-Aperture Color-Separation Gratings for Diverting Unconverted Light Away from the National Ignition Facility Target

S. N. Dixit
L. Auyang
I. M. Barton
J. A. Britten
S. M. Herman
T. Parham
M. D. Perry
M. C. Rushford
L. J. Summers
I. M. Thomas

Introduction

Most of the glass, laser-based inertial confinement fusion (ICF) systems around the world today employ nonlinear frequency conversion for converting the 1.053-μm light at the fundamental frequency (referred to as 1ω light) to either its second harmonic (2ω) at 527 nm or to its third harmonic (3ω) at 351 nm. Shorter wavelengths are preferred for laser fusion because of the improved coupling of the laser light to the fusion targets due to reduced fast-electron production at shorter wavelengths. The frequency conversion process, however, is only about 60 to 70% efficient, and the residual 30 to 40% of the energy remains at 1ω and 2ω frequencies. The unconverted light, if permitted to interact with the plasma surrounding the target, could seed the production of fast electrons and could also stimulate the scattering processes in the plasma, scattering the 3ω light into light of longer wavelengths. These processes could prove detrimental to the ICF process itself. It is therefore desirable to move the unconverted light away from the ICF target.

Different strategies have been adapted for diverting the unconverted light away from the fusion target. On the Nova laser system at Lawrence Livermore National Laboratory (LLNL) and on the Phebus laser system at Limeil, France, the chromatic aberration in the focusing lens is used to cast a shadow of a 15-cm-diam circular obscuration at the center of the near-field profile to prevent the 1ω and 2ω light from hitting the target located at the 3ω focus. Here, different focal lengths at the 1ω and 2ω wavelengths lead to scaled-down, quasi-far-field profiles of the input beam at the 3ω focal plane. The shadow of the obscuration then prevents the unconverted light from hitting the target. At the OMEGA laser system at the University of Rochester, the unconverted light is filtered out using the differing reflectivities of a multilayer turning mirror. In the proposed French Laser MegaJoule (LMJ) design, the unconverted light is prevented from entering the target chamber altogether by the use of high-efficiency diffraction gratings.

Earlier designs for the proposed National Ignition Facility (NIF) at LLNL employed a wedged final focusing lens to divert the unconverted 1ω and 2ω light away from the laser entrance hole and the outer surface of the hohlraum. The increased thickness of the glass in the ultraviolet (UV) beam path leads to a larger nonlinear B-integral, which can degrade the beam quality and focusability of the 3ω light. In addition, larger deflections of the 1ω and 2ω light (if needed) would demand an even thicker wedge on the lens, further exacerbating the B-integral problem.

Recently, we have proposed the use of a color-separation grating (CSG) to move the unconverted light away from the target in the NIF laser.[1] CSGs[2–6] offer a versatile approach to reducing and possibly eliminating the unconverted light at the target region. A CSG (shown schematically in Figure 1) consists of a three-level lamellar grating designed so that nearly all of the 3ω light passes through undiffracted while the residual 1ω and 2ω energy is diverted with high efficiency into higher diffraction orders. The diffraction angle is determined solely by the grating period. Because a CSG profile is only a few wavelengths deep, the CSG can be fabricated on a thinner optic. The reduced amount of fused silica in the beam path lowers the B-integral,

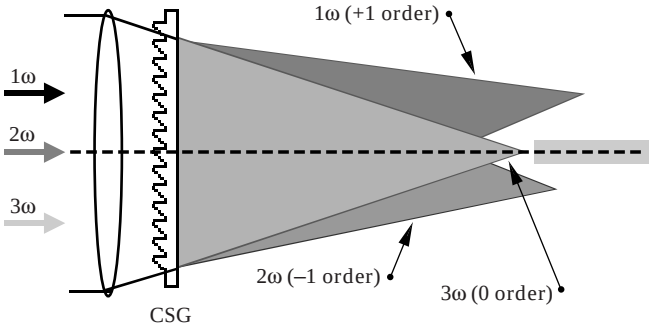

FIGURE 1. Schematic description of a CSG. For the sake of clarity, we have shown only the dominant diffraction orders for 1ω, 2ω, and 3ω wavelengths. In reality, the unconverted light is diffracted into several orders. (70-00-0598-1196pb01)

thereby reducing the nonlinear effects and consequently increasing the safety margin in the operation of high-power fusion lasers such as the NIF.

The current NIF baseline employs a CSG for diverting the unconverted light away from the target. Typical grating periods for NIF color separation are in the 300-μm range. The actual CSG grating period and the orientation of various CSGs on the NIF beams are still being determined. However, to demonstrate the technology of these CSGs, we have fabricated a 345-μm period CSG at the full-NIF aperture using a lithographic process similar to that used in the kinoform phase plate fabrication.[7] This CSG will be fielded in the upcoming experimental campaign on LLNL's Beamlet (a prototype of a single NIF beamline).

CSG Theory

In this section, we briefly outline the theory of CSGs and discuss the sensitivity of the CSG efficiency to various fabrication parameters. A schematic diagram of a CSG is shown in Figure 1. It consists of a three-level, staircaselike lamellar structure. Although CSGs consisting of more than three levels can be designed, a minimum of three levels is required to achieve the color separation functionality desired on the NIF. The height of each step is chosen so that a relative phase delay of 2π is introduced for the 3ω light. If d denotes the period of the grating, and λ the operating wavelength, then the angle of diffraction for the m^{th} order when light is incident normal to the CSG is given by the standard grating equation

$$\sin\left[\theta_m(\lambda)\right] = m\frac{\lambda}{d} \quad . \qquad (1)$$

Within the approximations of the scalar diffraction theory,[8] the diffraction efficiencies in various orders are given by the following equation

$$\eta_m = \left| \sum_{j=1-3} e^{-i\phi_j} \frac{n(\lambda)-1}{n(\lambda_0)-1} \frac{\lambda_0}{\lambda} e^{i2\pi m\varepsilon_j}\, \delta_j \operatorname{sinc}\left(\pi m \delta_j\right) \right|^2 \quad , \qquad (2)$$

where ϕ_j denotes the phase delay introduced due to the step j at the design wavelength λ_0 (351 nm), and ε_j and δ_j denote the locations of the center and the width of each zone within one CSG period. ε_j and δ_j are normalized to the grating period. For a regularly spaced grating, $\delta_j = 1/3$ for all j and $\varepsilon_j = 1/6$, $1/2$, and $5/6$ for $j = 1$, 2, and 3. The factors multiplying the phase ϕ_j account for the material dispersion and the chromatic dispersion due to the CSG profile.

If $\phi_j = 0$, 2π, and 4π for $\lambda_0 = 351$ nm, then the grating appears transparent to the 3ω light, and all the 3ω light passes through undiffracted in the zeroth-transmitted order. Interestingly enough, this three-level lamellar profile also implies a theoretical zeroth-order efficiency of zero for the 1ω and 2ω light in the absence of any material dispersion. The variation of the refractive index with wavelength leads to a small zeroth-order diffraction efficiency for 1ω and 2ω. Table 1 lists the theoretical diffraction efficiencies for a few orders around 0 and for 1ω, 2ω, and 3ω wavelengths. These results are based on the scalar

TABLE 1. CSG diffraction efficiencies in various orders (Eq. 2). Refractive index values for fused silica were used in these calculations. These are $n = 1.44976$, 1.46097, and 1.47672 at 1ω, 2ω, and 3ω respectively.

Diffraction order	1ω efficiency	2ω efficiency	3ω efficiency
–4	0.0002	0.0422	0
–3	0	0	0
–2	0.169	0.001	0
–1	0.003	0.675	0
0	0.005	0.006	1.0
1	0.678	0.005	0
2	0.0007	0.169	0
3	0	0	0
4	0.0422	0.0003	0

theory (Eq. 2), which is valid for grating periods much larger than wavelength. In this limit, the diffraction efficiencies are independent of the CSG period and are also insensitive to the polarization of the light.

It is clear from this table that about 88% of the 1ω light is diffracted into +1, –2, and +4 orders with the remaining energy distributed into many diffraction orders. The three-fold "skipping" of the diffraction efficiency is a consequence of the three-step structure in the CSG period. It is also interesting to note that, while the 2ω efficiencies are approximately the same as the 1ω efficiencies, the sign of the diffraction order is switched between 1ω and 2ω. This symmetry reversal results from the apparent reversal of the "blaze" between 1ω and 2ω. This can be understood as follows. Ignoring, for the simplicity of the argument, the material dispersion effects, the 0, 2π, and 4π phase delays at 3ω appear as 0, 2π/3, and 4π/3 at 1ω and 0, 4π/3, and 8π/3 at 2ω. Because integral multiples of 2π phase can be arbitrarily added to each step without affecting the optical performance, it can be shown that the step structure within a CSG period appears reversed for 2ω wavelength as compared to that for the 1ω wavelength. This is illustrated in Figure 2. This reversed "blaze" leads to a switching of the diffraction efficiencies to opposite orders among the 1ω and the 2ω light, as shown in Table 1.

Split Color-Separation Gratings

Eq. 1 indicates that the 1ω diffracted orders will have twice the angular spread as the 2ω diffracted orders. Unconverted light management on systems such as the NIF requires that the 1ω and 2ω light be moved a certain minimum distance away from the center. An improvement in the CSG designs can be achieved by reversing the lamellar CSG profile over half of the beam aperture, as shown in Figure 3. Such CSG profiles will be referred to as split CSGs. In this case, the dominant order for the 2ω light from each half of the beam is diffracted towards the same side, while that for the 1ω light "crosses" over to the opposite side. The larger deviation required to accommodate the crossover for the 1ω orders is provided by the larger 1ω diffraction angles. This translates into higher CSG periods for split CSGs to achieve a certain color separation compared to standard CSGs. For example, the CSG period required for moving the unconverted light footprints 1 cm away from the center is 243 μm for a standard CSG, while it is 381 μm for a split CSG. These CSG periods assume a 7.7-m focal length lens and a 400-mm near-field aperture for the beam. Larger CSG periods lead to lower fabrication errors, thereby leading to a higher CSG performance.

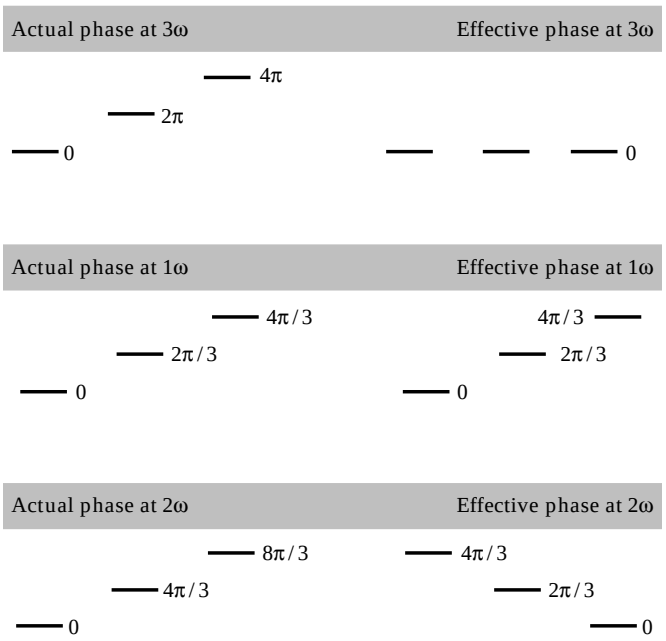

FIGURE 2. Effective CSG phase for the converted (3ω) and the unconverted (1ω and 2ω) light. Note that by adding multiples of 2π phase, it can be shown that the "blaze" of the staircaselike CSG profile appears reversed for 2ω light compared to 1ω light. (70-00-0598-1197pb01)

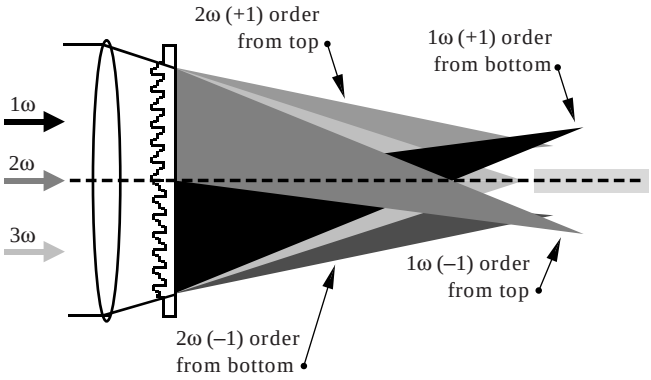

FIGURE 3. Schematic description of a split CSG. Note that the CSG profile is symmetric about the beam center. Again, for the sake of clarity, we have shown only the dominant diffraction orders for 1ω, 2ω, and 3ω wavelengths. In reality, the unconverted light is diffracted into several orders from the top and the bottom halves of the beam. (70-00-0598-1198pb01)

CSG Sensitivity to Fabrication Errors

The three-level CSG profile has to be fabricated using a two-mask lithographic process with either a wet etch or a dry etch into fused silica. The fabrication errors consist of errors in the etch depth and errors due to mask misalignment. Although the theoretical calculations above predict zeroth-order diffraction efficiency of unity for the 3ω light and nearly zero for the residual 1ω and 2ω light, fabrication errors in a practical application reduce the throughput at 3ω and increase the 1ω and 2ω zero-order light. Figure 4 displays the variation of the diffraction efficiency in the zeroth order with the etch depth error in the two steps. From these results we see that the etch depth has to be controlled to within ±20 nm to maintain desirable 3ω focusing (>98% without accounting for Fresnel losses) and color separation (<1%) characteristics.

The absolute etch depths required for each step of the CSG depend on its angle of use. In high-power laser systems, the diffractive optics are often used at off-normal angles of incidence to minimize ghost reflection issues. On the NIF, the CSG is planned to be used at 14° angle of incidence, whereas on Beamlet it will be used at 20 to 22°. The optical phase difference (OPD) between the etched and the unetched regions increases at small angles of incidence according to the formula

$$OPD \approx (n-1)t\left(1+\theta^2\frac{1}{2n}\right)\frac{2\pi}{\lambda} \quad , \tag{3}$$

where θ is the angle of incidence, n the refractive index of the substrate relative to air (which is assumed to have refractive index 1.0), and t the relative step height between the etched and the unetched regions. This implies that diffractive optics, when used at oblique angles, have to be etched thinner than for normal incidence use. This is illustrated in Figure 5, where we plot the 3ω zeroth-order efficiency vs the CSG use angle for various etch depths for the first step (the second step etch depth is assumed to be twice the first step for simplicity). A 14°-use-angle CSG, for example, has to have an etch depth of 700 to 740 nm to maintain >98% 3ω zero-order efficiency, while for a 20°-use-angle CSG it has to be in the range 680 to 720 nm.

An additional effect of using the CSG at an off-normal angle is a reduction in the effective grating period by the cosine of the angle of incidence. At a 14° angle of incidence, the effective CSG period is reduced by 3%, while at 22° it is reduced by 7%. This leads to a corresponding increase in the diffraction angles for various orders. If the diffracted orders are required to be propagating at specific angles, then the effect of the CSG tilt can be compensated for in the actual CSG period fabricated.

Mask misalignment and problems associated with undercutting during the lithographic fabrication of a CSG lead to an erosion of the sharpness of the edge between the various steps in the CSG. Types of erosion consist of a rounding off of the edge of the CSG grooves, a lateral shift in the location of the edge, a misaligned overlay, etc. Often more than one type of error occurs in a given fabrication process. The dominant effect of these

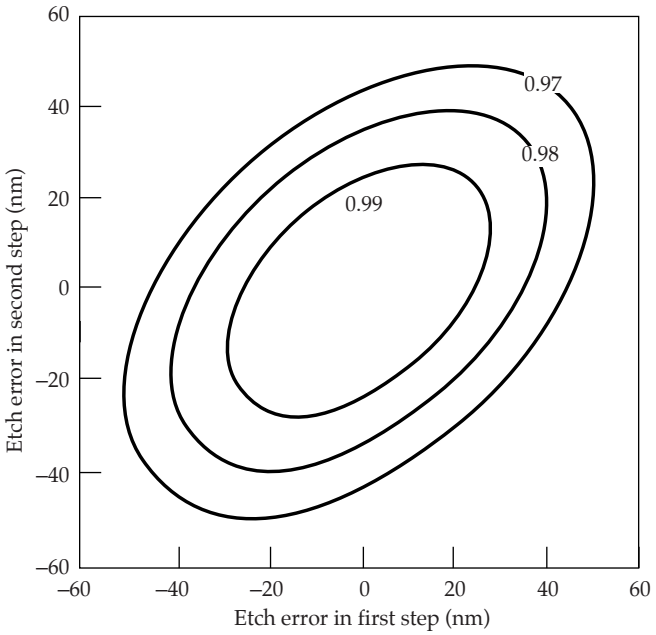

FIGURE 4. A contour map of the 3ω zeroth-order diffraction efficiency of a CSG as a function of the etch depth errors in the two steps. The values against each contour indicate the diffraction efficiency. (70-00-0598-1199pb01)

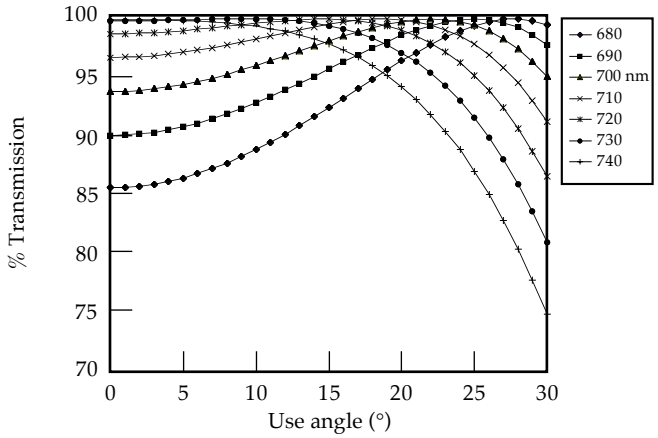

FIGURE 5. Effect of the use angle on the CSG 3ω transmission. Various curves correspond to different step heights for the 2π step. The 4π step is assumed to be twice as deep as the 2π step. (70-00-0598-1200pb01)

edge erosion errors is a loss of the 3ω zeroth-order efficiency. This loss can be simply estimated as the fractional area loss due to the edge degradation. Detailed calculations confirm this. The 3ω zeroth-order efficiency can then be written as

$$\eta_0 \approx \left|1-\frac{\Delta_1+\Delta_2+\Delta_3}{d}\right|^2 \approx 1-2\frac{\Delta_1+\Delta_2+\Delta_3}{d} \quad , \qquad (4)$$

where Δ_1, Δ_2, and Δ_3 denote widths of the eroded edges. Thus, good alignment and edge definition control are required for maintaining high 3ω throughput. For example, for a CSG with a 300-μm period, a 1-μm-wide edge rounding at each step leads to a 2% loss of efficiency due to edge erosion. It should be mentioned that the 1ω and 2ω zeroth-order efficiencies are less sensitive to the effects of edge degradation and etch depth errors.

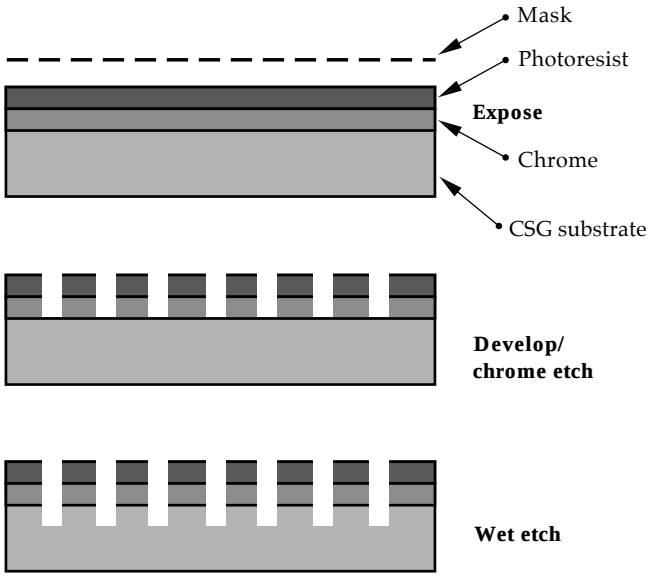

FIGURE 6. Schematic illustration of the various steps in the fabrication of a CSG by lithographic methods. (70-00-0598-1201pb01)

Fabrication of a Full-Aperture CSG for the Beamlet Laser

To demonstrate the concept of unconverted light management using CSGs, we fabricated a standard CSG having a 345-μm period in a Beamlet-size fused silica substrate (~400 × 400 mm) using a lithographic process and wet-etching process.[7,9] This particular CSG period was chosen because we had previously fabricated CSGs at this period at smaller apertures[1] and also because this period is of the same magnitude required for the baseline NIF operation. The CSG fabrication method is schematically illustrated in Figure 6. The CSG substrate is first coated with a thin layer of chrome, and a layer of photoresist is deposited over it. This photoresist layer is then exposed to UV light from an arc lamp through a binary (in transmission) photomask. The exposed photoresist is developed away, and the chrome layer in these areas is removed using a chrome etch. This clears areas on the fused silica substrate that are subsequently etched in a buffered hydrofluoric acid solution. The etch depth is controlled by the time duration of the etch. Following the etching to a desired depth, the remaining photoresist is washed off. At this step, one set of the CSG grooves has been fabricated. This entire sequence of steps is repeated for a second time with a second photomask to etch the second set of steps in the CSG substrate. The second mask pattern is aligned carefully to the first etched pattern in the substrate by using a set of precisely located alignment fiducials. Finally, at the end of the sequence of steps using the second mask, the remaining chrome (over the grooves corresponding to zero phase) is etched off.

The binary photomasks required for the CSG fabrication were patterned in a chrome layer coated over a fused silica substrate using the large-aperture photoplotter developed at our laboratory. The available plotting area for the photoplotter is about 1 × 1 m sq. The pixel positioning and the pixel size are accurate to ~0.5 μm each over the entire plotting area. We believe that the edge definition through the sequence of the lithographic steps mentioned above erodes to ~1.5 μm. This leads to an ~2.5% reduction in the 3ω zeroth-order throughput.

We tried to achieve the desired etch depths of 720 and 1440 nm for the two CSG steps by first etching to 80% of the desired value, measuring the step height in a few selected places on the substrate, and then completing the remaining etch using an adjusted (if needed) etch rate. The etch depths on the finished parts were in the range of 704 to 743 nm (for the 2π steps) but varied somewhat over the 40-cm part. We believe this is due to a variation in the surface quality on the substrate that, as we shall see below, affects the uniformity of the 3ω diffraction efficiency.

Optical Performance

We characterized the optical performance of the CSG by measuring the zeroth-order transmission efficiencies 1ω, 2ω, and 3ω light. These measurements were carried out by scanning the full-size optic across an ~5-mm collimated beam and collecting the transmitted light. The optic was not antireflection (AR) coated for these

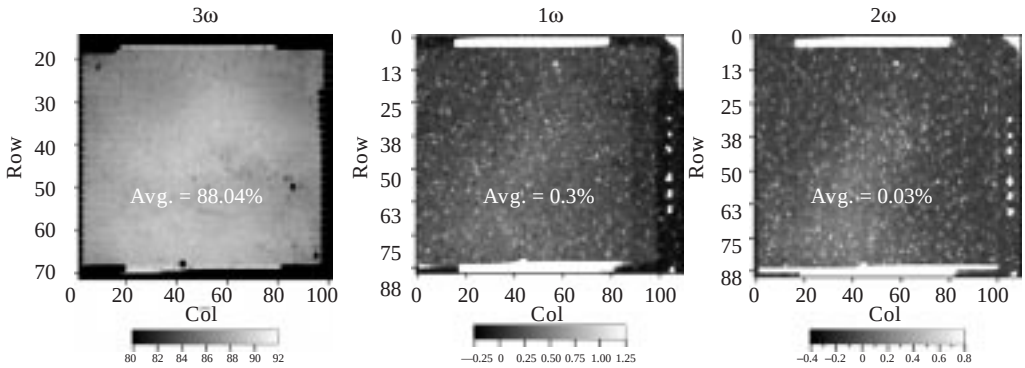

FIGURE 7. Measured 1ω, 2ω, and 3ω zeroth-order transmission of a full-aperture (40-cm-sq) CSG. These measurements were carried out at 22° angle of incidence. The substrate was not AR-coated in these measurements. (70-00-0598-1202pb01)

measurements. The measured transmission efficiencies are shown in Figure 7. We see from this data that excellent 1ω and 2ω suppression (<1% for each color) is achieved while the 3ω zero-order transmission is in the range of 86 to 89%, with an average value of 88%. Note that the 3ω transmission of an uncoated fused silica flat substrate is 92.5%. When normalized to this value, we can deduce that the normalized CSG efficiency is about 95%. Considerable variation of the 3ω zeroth-order transmission is observed across the 40-cm aperture. Through the measurements of the etched step heights using a white light interferometer, we have been able to qualitatively correlate the transmission efficiency nonuniformities to variations in the etch depth. We believe that the physical reason for this variation is an etch rate nonuniformity across the sample possibly introduced during the finishing process. The measured etch depths together with the data in Figure 5 indicate that at the NIF use angle of 14°, the expected variations in the 3ω zeroth-order transmission efficiency would be reduced. This was verified by measuring the transmission of this CSG at 13°. The results, shown in Figure 8, indicate that diffraction efficiencies at this angle are in the range of 89 to 91%, with an average value of 90.7%. When normalized to the uncoated fused silica transmission (92.5%), we obtain a CSG efficiency of 98%.

Effect of Sol-Gel AR Overcoating on the CSG Performance

Optics used in high-power fusion lasers such as Nova and NIF are AR coated with an LLNL-developed sol-gel colloidal silica coating[10] to increase the transmission efficiency. We AR coated a previously fabricated CSG using the dip-coating process normally used to coat Nova and NIF parts. We observed that when the CSG surface was AR coated, the transmission efficiency in the zero order was reduced compared to leaving the CSG surface bare. We found that the AR overcoating the CSG surface causes light to be scattered into the higher-transmitted diffractive orders to a greater extent than it reduces the back-reflection losses. This effect is shown in Figure 9. Approximately 7 to 10% of the total incident light is

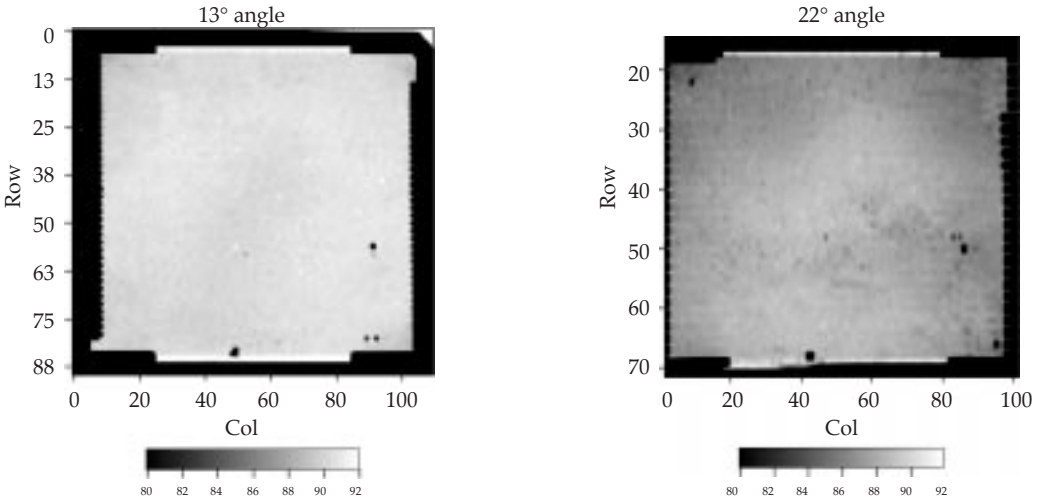

FIGURE 8. A comparison of the 3ω zeroth-order transmission efficiencies at 13° and at 22° angles of incidence. Note the increased transmission value as well as its uniformity at 13° angle of incidence. (70-00-0598-1203pb01)

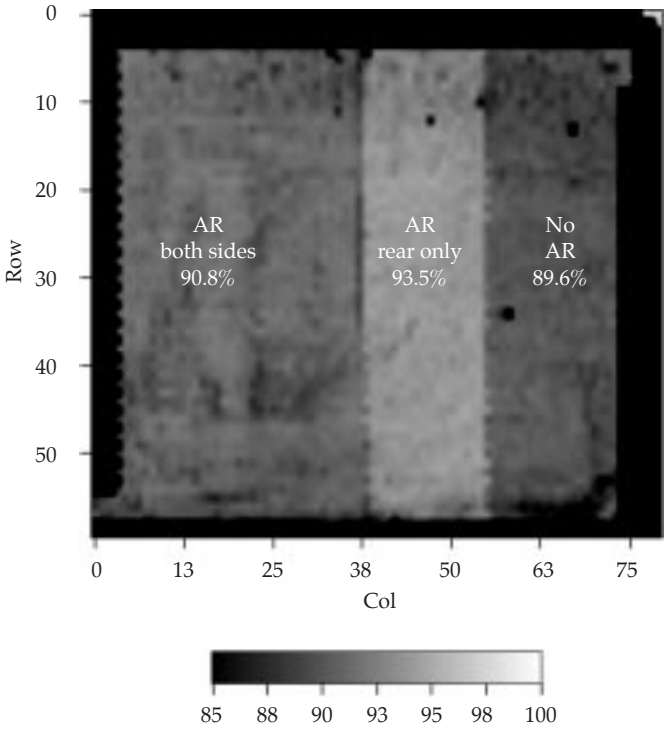

FIGURE 9. Effect of dip-coated porous silica antireflection coating on the 3ω zeroth-order transmission. The entire optic was dip-coated, and portions of the AR coating were stripped off from one or both sides to understand the effect of the AR coating on the CSG performance. (70-00-0598-1204pb01)

directed into the higher-transmitted diffracted orders by this coating, whereas losses into these orders are 2 to 3% for the bare surface. It is worth noting, however, that the zero-order transmission of 1ω and 2ω light is not affected by the AR coating.

Optical microscopy and detailed photometric examination of the amount of light scattered into individual higher-transmitted orders lead to the conclusion that these losses are due to a partial planarization effect of the coating. The coating is applied from liquid suspension by dip coating, a process in which liquid surface tension plays a crucial role. In the vicinity of the edges of the CSG pattern, surface tension effects cause a lateral flow of the liquid film during drying, which partially fills in and rounds the edges of the coated layer, as illustrated in Figure 10. This nonuniformity extends for several micrometers out into the grating line, in effect introducing a net sidewall slope error that, according to calculations, is sufficient to account for the measured zero-order losses.

This surface-tension effect is inherent in the dip-coating process and cannot be mitigated by, for example, changing solvents. The effect of surface tension on planarization is much less, however, for application of the AR coating by a spin-coating process. Preliminary data suggests that spin-coating of the same sol-gel AR

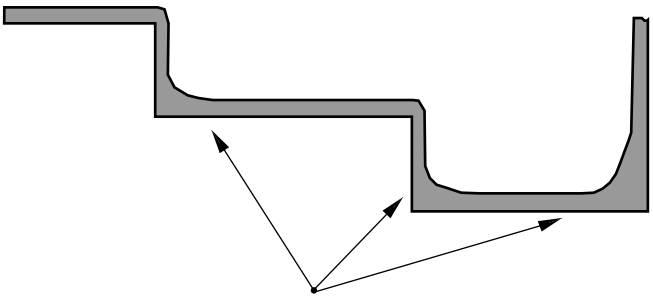

FIGURE 10. Schematic illustration of the planarization of the AR coating around the edges of a CSG. The rounded corners lead to a degradation of the CSG efficiency. (70-00-0598-1205pb01)

coating can achieve zero-order transmission efficiencies equal to or slightly better than the 95% NIF specification, although it is not as good as a completely conformal AR coating would be. Conformal coatings are possible if applied by vacuum deposition processes using refractory dielectric materials. Historically, these coatings have not been shown to have the required laser damage resistance, but improvements in the damage resistance of these types of coatings is ongoing. We are continuing to investigate the potential of spin coating the full-aperture CSG using the sol-gel system as well as evaluating the laser damage thresholds of possible hard-coat AR coatings.

Conclusions

In summary, we have designed and fabricated a CSG at NIF aperture sizes for use on the Beamlet laser. When the CSG is uncoated, its normalized optical performance is close to the expected values (>97% transmission in 3ω zeroth order without accounting for Fresnel losses and <1% in the 1ω and 2ω zeroth orders). We have observed an ~7 to 10% degradation in the 3ω transmission when the substrate is AR coated, and we are currently investigating its causes and possible solutions.

References

1. S. N. Dixit et al., *SPIE* **3047**, 463–470 (1997).
2. H. Dammann, *Appl. Opt.* **17**, 2273–2279 (1978).
3. T. Bett and I. Barton, private communication (AWE Aldermaston, Reading, UK).
4. M. B. Stern and G. J. Swanson, "Color separation echelon gratings," in *1996 Technical Digest Series*, vol. 5, Optical Society of America, April 1996.
5. M. W. Farn et al., *Opt. Lett.* **18**, 1214 (1993).
6. M. W. Farn et al., *NASA Conf. Publ.* **3227**, 409 (1993).
7. M. C. Rushford et al., *SPIE* **3047**, 282–291 (1997).
8. J. W. Goodman, *Introduction to Fourier Optics*, (McGraw Hill, New York, NY, 1988), p. 67.
9. S. N. Dixit et al., *Appl. Optics* **32**, 2543 (1993).
10. I. M. Thomas, *Appl. Optics* **25**, 1481 (1986).